

Synthesis of ZnO Nanoparticles with Tunable Emission Colors and Their Cell Labeling Applications

Xiaosheng Tang, Eugene Shi Guang Choo, Ling Li, Jun Ding, and Junmin Xue*

Department of Materials Science and Engineering, National University of Singapore, Blk E3A, 04-10,
7 Engineering Drive 1, Singapore 117574

Received December 28, 2009. Revised Manuscript Received April 21, 2010

ZnO nanoparticles have been studied for potential cell labeling applications over the past several years. However, little progress has been made because of the limited emission color and poor water stability of ZnO nanoparticles. In this work, ZnO nanoparticles with various emission colors, including blue, green, yellow, and orange, were synthesized through an ethanol-based precipitation method. The emission color of the ZnO nanoparticles could be tuned by adjusting the pH value of the precipitation solution. The as-prepared ZnO nanoparticles were then encapsulated with silica to form ZnO@silica core shell nanoparticles, to improve the water stability of the ZnO nanoparticles. The visible emissions of the ZnO nanoparticles were well retained after they had been coated with silica shells. The resultant ZnO@silica core shell nanoparticles exhibited low cytotoxicity and were promising in cell labeling applications.

1. Introduction

Fluorescent probes have been widely used to study cellular morphology, behavior, and physiological functions. To achieve high-quality imaging and tracking of biological cells, these probes should be water-dispersible and biocompatible, with a high luminescent efficiency. In the past century, organic dyes and fluorescent proteins were the major fluorescent probes used for biological and biomedical research.¹ However, these organic probes are highly susceptible to photobleaching, so they are not suitable for long-term cell imaging applications.² This shortcoming has led to a strong interest in colloidal fluorescent semiconductor quantum dots (QDs), which have shown to be promising for cell imaging since 1998.³ The toxicity of QDs has been widely studied, but the mechanisms of the toxicity are still in question. The release of heavy metal ions such as Cd²⁺ is frequently proposed to explain the toxicity of QDs,⁴ but recent studies

have also demonstrated that the surface chemistry and production of reactive oxygen species (ROS) from QDs play a crucial role in their toxicity.⁵ Besides the toxicity concern, producing and employing heavy metal ion-based compounds are harmful to human health and pose a potential environmental hazard. With regard to the inherent problems of heavy metal ion-based QDs, the search for new cellular probes has become increasingly urgent and important.

Recently, much attention has been paid to an alternative semiconductor, ZnO, for cell labeling applications.⁶ In principle, ZnO nanoparticles do not have any visible excitonic emission as their band gap is 3.4 eV,⁷ which is beyond the visible wavelength range. Interestingly, it has been observed that the freshly prepared ZnO nanoparticles are able to emit green light under UV excitation and thus are interesting for cell labeling applications. Although much effort has been spent in developing ZnO into a new cell labeling probe, the fact that little progress has been made to date was unexpected. Generally, there are two major problems with ZnO in cell labeling applications. The first problem arises from their limited emission color. It is believed that the visible green emission of ZnO nanoparticles is attributed to their surface defects;⁸ however, these surface defects have not been well-defined so far, and the correlation between the surface defects and the visible emission is not yet

*To whom correspondence should be addressed. Fax: +65 6776 3604. Telephone: +65-6516 4655. E-mail: msxuejm@nus.edu.sg.

- (1) Alivisatos, A. P. *Science* **1996**, *271*, 933.
- (2) Tang, Z.; Kotov, N. A.; Giersig, M. *Science* **2002**, *297*, 237.
- (3) (a) Chan, W. C. W.; Nie, S. *Science* **1998**, *281*, 2016. (b) Peng, X.; Manna, U.; Yang, W.; Wickham, J.; Scher, E.; Kadavanich, A.; Alivisatos, A. P. *Nature* **2000**, *404*, 59. (c) Han, M.; Gao, X.; Su, J. Z.; Nie, S. *Nat. Biotechnol.* **2001**, *19*, 631.
- (4) (a) Hines, M. A.; Guyot-Sionnest, P. *J. Phys. Chem.* **1996**, *100*, 468. (b) Wood, A.; Giersig, M.; Hilgendorff, M.; Vilas-Campos, A.; Liz-Marzan, L. M.; Mulvaney, P. *Aust. J. Chem.* **2003**, *56*, 1051. (c) Abdullah, M.; Shibamoto, S.; Okuyama, K. *Opt. Mater.* **2004**, *15*, 1751. (d) Wu, Y. L.; Lim, C. S.; Fu, S.; Tok, A. I. Y.; Lau, H. M.; Boey, F. Y. C.; Zeng, X. T. *Nanotechnology* **2007**, *18*, 5604. (e) Jamieson, T.; Bakhshi, R.; Petrova, D.; Pocock, R.; Imani, M.; Seifalian, A. M. *Biomaterials* **2007**, *28*, 4717. (f) Hardman, R. *Environ. Sci. Technol.* **2008**, *42*, 6264.
- (5) (a) Schneider, R.; Wolpert, C.; Guilloteau, H.; Balan, L.; Lambert, J.; Merlin, C. *Nanotechnology* **2009**, *20*, 225101. (b) Dumas, E.; Gao, C.; Suffern, D.; Bradforth, S. E.; Dimitrijevic, N. M.; Nadeau, J. L. *Environ. Sci. Technol.* **2010**, *44*, 1464.

- (6) Xiong, H.; Wang, Z.; Liu, D.; Chen, J.; Wang, Y.; Xia, Y. *Adv. Funct. Mater.* **2005**, *15*, 1751.
- (7) (a) Jin, J.; Soon, G. K.; Jung, H. Y.; Taeghwan, H. *Adv. Mater.* **2005**, *17*, 1873. (b) Chen, Y.; Myeongseob, K.; Lian, G.; Mathew, B. J.; Peng, X. *J. Am. Chem. Soc.* **2005**, *127*, 13331. (c) Tamar, A.; Gong, Y.; Polking, M.; Yin, M.; Igor, K.; Gertrude, N.; Stephen, O. B. *J. Phys. Chem. B* **2005**, *109*, 14314. (d) Narayanaswamy, A.; Xu, H.; Pradhan, N.; Kim, M.; Peng, X. *J. Am. Chem. Soc.* **2006**, *128*, 10310.
- (8) (a) Xiong, H.; Xu, Y.; Ren, Q.; Xia, Y. *J. Am. Chem. Soc.* **2008**, *130*, 7522. (b) Moussodia, R. O.; Balan, L.; Merlin, C.; Mustin, C.; Schneider, R. *J. Mater. Chem.* **2010**, *20*, 1147.

clear. Several attempts have been made to tune the emission color of ZnO nanoparticles through surface modifications. For instance, it was reported that various color emissions of ZnO nanoparticles could be achieved by surface modification with polymers,⁸ but the mechanisms of the various color emissions through these polymer surface modifications are far from being understood. To date, tuning the emission color of ZnO nanoparticles remains challenging because of the lack of a known exact mechanism.

Besides the limited emission color, ZnO shows poor stability in water, and this poses the second serious problem with ZnO nanoparticles as cell labeling probes. It has been well documented that the equilibrium concentration of Zn^{2+} in water is quite high over a wide pH range.⁷ This allows the as-prepared ZnO nanoparticles to be dissolved in water easily over a wide pH range. It is possible to stabilize ZnO nanoparticles in water through surface modifications, but this is usually at the cost of losing their original visible green emission. For example, Liu et al. reported that ZnO nanoparticles could be stabilized by being coated with diethanolamine (DEA) and oleic acid (OA).⁹ The resultant ZnO nanoparticles could demonstrate visible blue emission only at 430 nm, which is not ideal for biological labeling because most cells and tissues also appear blue under UV light.

Although there is still much to understand about the mechanisms for visible emission of ZnO nanoparticles, numerous research reports have revealed that the surface oxygen vacancies play an important role in the visible emission of ZnO.^{6,8,9} The surface oxygen vacancies are also related to the surface-bound OH^- and H^+ groups. By modifying the surface-bound OH^- or H^+ groups through pH value adjustment, we may be able to optimize the surface oxygen vacancies and then tune the emission color of ZnO nanoparticles. On the basis of this understanding, a precipitation process was designed to synthesize ZnO nanoparticles with tunable emission colors. With this method, no other additives such as surfactants or polymers were added except for zinc acetate and lithium hydroxide (LiOH). ZnO nanoparticles were prepared by precipitation of Zn^{2+} purely with LiOH in ethanol. Our experimental results showed that ZnO nanoparticles with various emission colors were successfully created via adjustment of the concentration of LiOH. However, the as-precipitated ZnO nanoparticles were not stable in water for a long period of time. To stabilize the ZnO nanoparticles in water, the as-precipitated ZnO nanoparticles were then encapsulated with silica to form ZnO@SiO_2 silica core shell nanostructures. Silica was selected as the shell material because of its biocompatibility, water stability, and rich surface chemistry.¹⁰ The obtained ZnO@SiO_2 silica core shell nanoparticles exhibited excellent water stability, and the visible emissions of ZnO were retained.

The cell labeling applications of the created ZnO@SiO_2 nanoparticles are also demonstrated in this work.

2. Experimental Section

Raw Materials. Lithium hydroxide (LiOH, 99% pure, Sigma-Aldrich), sodium hydroxide (NaOH, 99% pure, Sigma-Aldrich), potassium hydroxide (KOH, 99% pure, Sigma-Aldrich), calcium hydroxide [$\text{Ca}(\text{OH})_2$, 99% pure, Sigma-Aldrich], zinc acetate (99% pure, Sigma-Aldrich), ethanol (absolute, Sigma-Aldrich), tetraethoxysilane (TEOS, 99% pure, Sigma-Aldrich), 3-[2-(aminoethyl)aminopropyl]trimethoxysilane (APTS, 99% pure, Sigma-Aldrich), dimethyl sulfoxide (DMSO, 99% pure, Sigma-Aldrich), and ultrapure water (18 M Ω cm) were used without further purification.

Synthesis of ZnO Nanoparticles. ZnO nanoparticles were prepared through a precipitation method by using LiOH as the precipitation agent in ethanol. In general, 0.2 mmol of zinc acetate was dissolved in 20 mL of absolute ethanol. The mixture was dissolved completely by being stirred at room temperature for 30 min; 36 mg of LiOH was dissolved in 20 mL of absolute ethanol. The zinc acetate/ethanol solution was then added to the LiOH/ethanol solution. The pH value of the solution was measured to be 12. After reaction for 2 h, the solution became turbid, indicating ZnO nanoparticles were formed. The pH values of the solutions were tuned to 10, 8, and 6 when 14, 10, and 5.5 mg of LiOH were added, respectively. The obtained ZnO nanoparticles that precipitated at different pH values were first washed using absolute ethanol to remove unreacted precursors, and the washing process was repeated three times. The purified nanoparticles were then dispersed in absolute ethanol for storage.

Synthesis of ZnO@SiO_2 . Twenty milliliters of an ethanol solution containing 0.25 mmol of ZnO nanoparticles and 0.06 mL of tetraethoxysilane (TEOS) were added to 4 mL of a water solution, and then the solution was treated with ultrasound for 10 min. Subsequently, 5 mg of ammonia dissolved in 10 mL of ethanol was added slowly to the solution with continuous stirring. The pH value of the solution was 8. The solution was transferred to a 100 mL cone-shaped beaker and stirred for 24 h under a nitrogen atmosphere. The solution was then centrifuged at 3000 rpm for three cycles. The purified particles were then dispersed in absolute ethanol for storage.

Surface Modification of ZnO@SiO_2 . Five milliliters of ZnO@SiO_2 nanoparticles in ethanol was taken, and an additional 25 mL of ethanol containing 100 μL of 3-[2-(aminoethyl)aminopropyl]trimethoxysilane (APTS) was added. After being stirred for 10 h, the solution described above was heated to reflux for 1 h. Then APTS-modified ZnO@SiO_2 nanoparticles were collected through centrifugation, washed with ethanol several times, and finally dispersed in water.

Cell Labeling. NIH/3T3 cells were placed in a 96-well plate and incubated at 37 °C in 5% CO_2 in air. After 24 h, 10 μL of ZnO@SiO_2 nanoparticles at 10 $\mu\text{g/mL}$ was injected into each well. The particles were then incubated for 24 h at pH 7.4. After incubation, the cells were observed using an Olympus Ix2-DSU disk scanning confocal microscope.

MTT Assay for Cytotoxicity of ZnO@SiO_2 Nanoparticles. The MTT solution was filtered through a 0.22 μm filter and stored at 4 °C. NIH/3T3 cells were divided into a 96-well plate at a density of 4000 cells per well and were incubated with ZnO@SiO_2 nanoparticles at different concentrations for 24 h. Following this, 10 μL of MTT was added to each well. After incubation at 37 °C for ~2–3 h in 5% CO_2 in air, the cell culture

- (9) Fu, Y.; Du, X.; Sergei, A. K.; Qiu, J.; Qin, W.; Li, R.; Sun, J.; Liu, J. *J. Am. Chem. Soc.* **2007**, *129*, 16029.
 (10) (a) Lu, Y.; Ying, Y. D.; Mayers, B. T.; Xia, Y. N. *Nano Lett.* **2002**, *2*, 183. (b) Deng, Y. H.; Wang, C. C.; Hu, J. H.; Yang, W. L.; Fu, S. K. *Colloids Surf., A* **2005**, *252*, 87. (c) Li, L.; Choo, E. S. G.; Yi, J. B.; Ding, J.; Tang, X. S.; Xue, J. M. *Chem. Mater.* **2008**, *20*, 6292. (d) Li, Z. Q.; Zhang, Y. *Angew. Chem., Int. Ed.* **2006**, *45*, 7732.

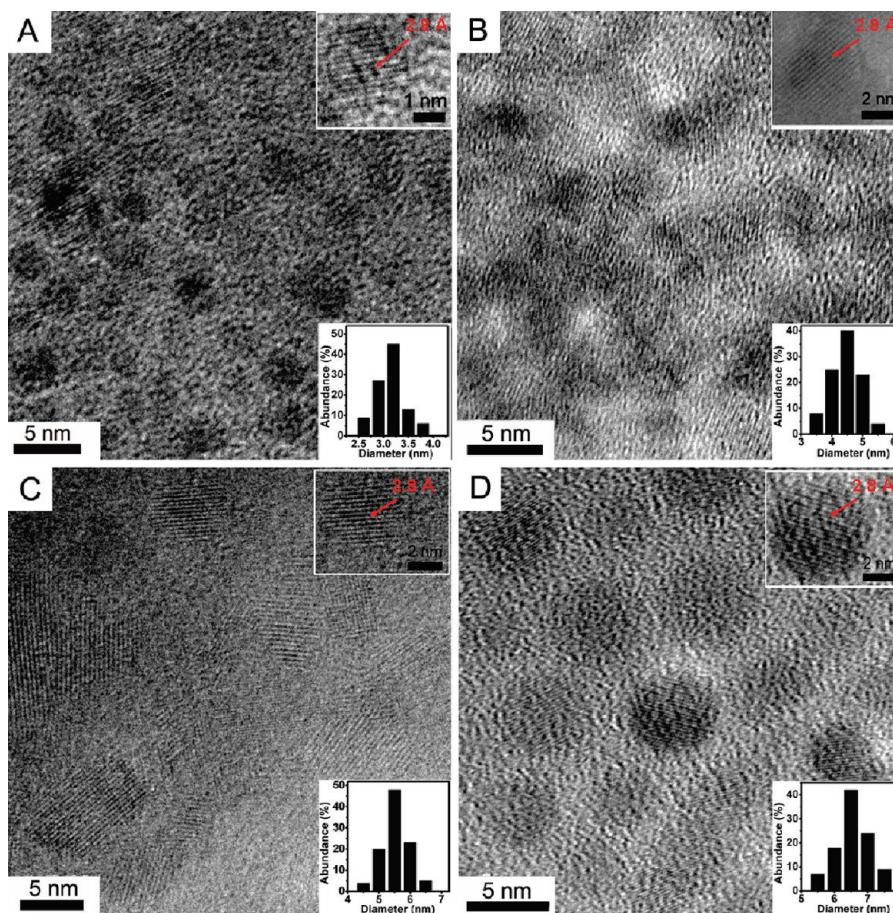


Figure 1. TEM images of ZnO nanoparticles that precipitated in ethanol at pH (A) 12, (B) 10, (C) 8, and (D) 6. In each panel, the top right inset shows the HRTEM image of a single nanocrystal and the bottom right inset the histogram of size distribution.

medium was removed with a needle and syringe. The wells were washed three times using PBS, and then 200 μ L of DMSO was added to each well. After \sim 2 h, the plate was analyzed using a microplate reader.

Characterizations. All transmission electron microscopy (TEM) images were obtained using JEOL 100CX instrument (200 kV). We prepared samples by dipping carbon-coated copper grids into the sample solution and then drying them at room temperature. Photoluminescence (PL) spectra were recorded in open-sized 1 cm path-length quartz cuvettes using a Perkin-Elmer LS 55 spectrofluorometer. UV-vis absorption spectra were recorded on a UV-1601 spectrophotometer.

3. Results and Discussion

ZnO nanoparticles were precipitated in ethanol at pH 12, 10, 8, and 6. The pH value was adjusted by modifying the concentrations of LiOH added. The TEM images and size distribution histograms of the resultant ZnO nanoparticles are presented in Figure 1. When the pH value is 12, as shown in Figure 1A, the obtained ZnO nanoparticles were well dispersed and their particle size ranged from 2 to 5 nm with an average particle size of 3.3 nm. Lattice fringe was clearly observed in the HRTEM image of a single ZnO nanoparticle, and the lattice space was 2.8 Å (inset of Figure 1A), which corresponds to the distance between two (0002) planes of ZnO. The particle size of ZnO nanoparticles was slightly increased when the pH

value was decreased. As shown in Figure 1B, the average size of the precipitated ZnO nanoparticles at pH 10 was \sim 4.5 nm. The particle size of the precipitated ZnO nanoparticles was continuously increased when the pH value was further decreased, i.e., 5.5 nm at pH 8 and 6.5 nm at pH 6 (Figure 1C,D). The resultant ZnO nanoparticles at pH 8 and 6 were well-crystallized as indicated by their respective HRTEM image. In this ethanol-based precipitation method, it is clear that pH value is a key factor in controlling the size of the ZnO nanoparticles. At a high pH value, ZnO nuclei were formed faster and in a larger amount than those at a low pH value. This led to competition growth of ZnO nanoparticles at a high pH value and thus resulted in the smaller particle size. The SAED patterns of ZnO nanoparticles that precipitated at different pH values were determined, and the results are shown in Figure S1 of the Supporting Information. All the diffraction rings in the SAED patterns were ascribed to the lattices of ZnO nanocrystals.

Figure 2A shows the photoluminescence (PL) spectra of the ZnO nanoparticles that precipitated at pH 12, 10, 8, and 6, which were labeled as samples A–D, respectively. We observed that the PL excitation peak of the samples was shifted increasingly from 309 to 356 nm when the precipitation pH value was decreased from 12 to 6. The red shift of the PL excitation with a decrease in pH value could be ascribed to the quantum confinement effect.

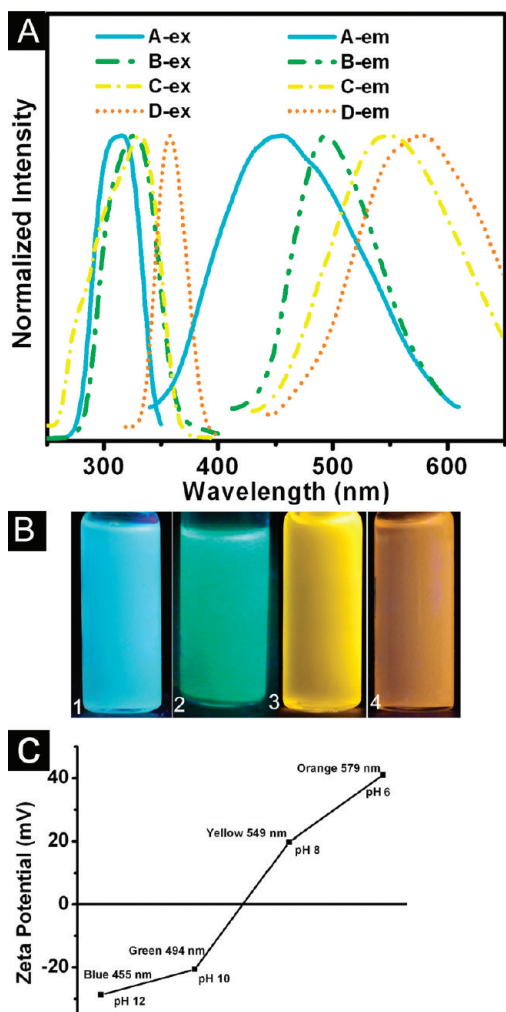
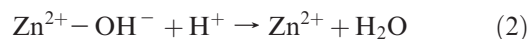
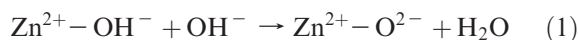


Figure 2. (A) Photoluminescent spectra of the ZnO nanoparticles that precipitated at pH (A) 12, (B) 10, (C) 8, and (D) 6. The ZnO nanoparticles were dispersed in ethanol. The excitation wavelengths were 309, 325, 328, and 356 nm for the nanoparticles prepared at pH 12, 10, 8, and 6, respectively. (B) Corresponding photographs of ZnO nanoparticles prepared at pH (1) 12, (2) 10, (3) 8, and (4) 6 under 365 nm excitation. (C) ζ potentials of ZnO nanoparticles that precipitated at different pH values.

The particle size of the ZnO nanoparticles tended to be larger with a decreasing pH value and thus led to a decrease in the band gap energy and an increase in the absorption wavelength. The similar quantum confinement effects of ZnO nanoparticles have been reported previously.^{6,8} More interestingly, ZnO nanoparticles precipitated at different pH values presented various visible color emissions in ethanol under their respective peak UV excitations. For instance, when the precipitation pH value was 12, the ZnO nanoparticles exhibited blue emission at 455 nm under 309 nm excitation. The emission color could be tuned to green (494 nm, under 325 nm excitation), yellow (570 nm, under 328 nm excitation), or orange (590 nm, under 356 nm excitation) when the precipitation pH values were adjusted to 10, 8, or 6, respectively. The PL quantum yields (QY) of the ZnO nanoparticles were measured as compared to the standard rhodamine 6G ethanol solution (QY = 95%). The quantum yields of the blue, green, yellow, and orange emissions were 26.2, 30.1, 34, and 19%, respectively, as

shown in Figure S2 of the Supporting Information. The quantum yields of the ZnO nanoparticles obtained in this work are comparable with the quantum yield results reported by Xia et al.^{8a} However, the quantum yields of this work are lower than the quantum yield achieved in Schneider's work.^{8b} As reported in ref 8b, the quantum yield of ZnO nanoparticles could reach 59% with polymer surface modification. Figure 2B shows a photograph taken with a digital camera, showing that the obtained ZnO nanoparticles were dispersed in ethanol very well. Upon UV 365 nm illumination, various visible color emissions, such as blue, green, yellow, and orange, were observed for the ZnO nanoparticles that precipitated at pH 12, 10, 8, and 6, respectively.

It appeared that the visible emission of ZnO nanoparticles also underwent a red shift with an increase in particle size due to the quantum confinement effect. However, this should not be the case here as the visible emission of ZnO nanoparticles is not generated from the transfer of an electron from the conduction band to the valence band. Although the mechanisms of ZnO visible emission are still under debate, much previous research suggested that ZnO visible emission is the result of the transitions involving trapped levels, and that surface oxygen vacancies play an important role in the formation of these trapped levels.^{6,8} The surface charges of the ZnO nanoparticles at different pH values were then measured, and the results are presented in Figure 2C. When the pH was 12, the surface charge was -30 mV. With a decrease in the pH value, the surface charge became more positive, i.e., -28 mV at pH 10, 5 mV at pH 8, and 15 mV at pH 6.



The surface charge of oxides in solution is determined by the interaction between a surface-attached OH^- group and OH^- or H^+ groups in the surroundings, depending on the isoelectric point of the oxides. When the pH value is above the isoelectric point, the resultant oxides appear to have a negative charge because of the formation of O^{2-} on the surface (eq 1), and vice versa, the surface charge is positive due to the formation of Zn^{2+} below the isoelectric point (eq 2). From the surface charge results of ZnO nanoparticles shown in Figure 2C, we estimated that the isoelectric point of ZnO nanoparticles in this work was between 8 and 10. From the analysis presented above, we could induce that the ZnO surfaces were dominated by O^{2-} ions (less oxygen vacancy) at pH 12 and 10, while the surfaces were dominated by Zn^{2+} (more oxygen vacancy) at pH 8 and 6. Therefore, we determined that the wavelength of the visible emission of ZnO nanoparticles was increased (from blue to orange) with an increase in surface oxygen vacancy. We have to say that this conclusion was very phenomenon-based, but it at least provided useful information for the mechanistic studies of ZnO visible emission. We have also used KOH, NaOH, and $\text{Ca}(\text{OH})_2$ to precipitate ZnO

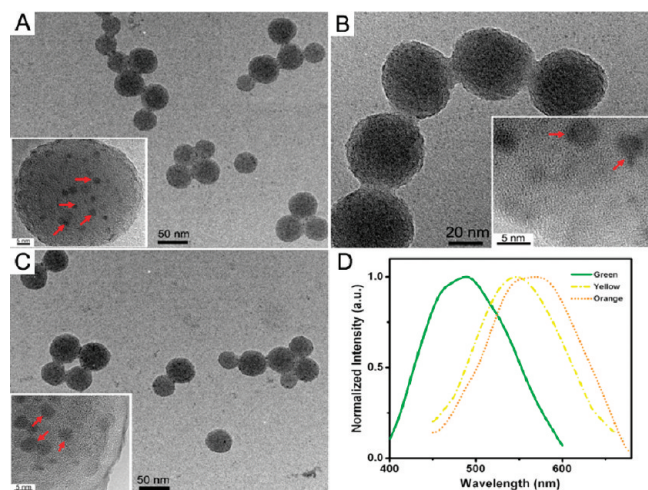


Figure 3. (A) TEM image of ZnO@silica core shell nanospheres. ZnO was prepared at pH 10. The inset is the high-magnification image of a single nanosphere. (B) TEM image of ZnO@silica core shell nanospheres. ZnO was prepared at pH 8. The inset is the high-magnification image of a single nanosphere. (C) TEM image of ZnO@silica core shell nanospheres. ZnO was prepared at pH 6. The inset is the high-magnification image of a single nanosphere. We prepared all the TEM samples of the ZnO@silica core shell nanoparticles by dipping carbon-coated copper grids into the sample solution and then drying them at room temperature. (D) Photoluminescent spectra of the three types of ZnO@silica nanospheres in water (excitation wavelength of 365 nm), showing that the PL properties of the ZnO nanoparticles were well retained after they had been coated with silica.

nanoparticles in ethanol solutions. We demonstrated that various visible color emissions could also be achieved by adjusting their respective concentrations, as shown in Figure S3 of the Supporting Information.

The ZnO nanoparticles with various visible color emissions are certainly interesting for cell labeling applications. However, the resultant ZnO nanoparticles, which precipitated in ethanol, were not stable in water. As shown in Figure S4 of the Supporting Information, visible emissions of the ZnO nanoparticles degraded fast when the particles were transferred from ethanol to water. It was believed that the degradation in visible emission was due to the corrosion of the nanoparticle surface in water. Therefore, it is of utmost importance to protect the nanoparticle surface by forming a chemically stable coating. The surface coating should also enhance the hydrophilicity and confer colloidal stability on the ZnO nanoparticles in water. In this work, the ZnO nanoparticles, which were precipitated at pH 10, 8, and 6, were then encapsulated with silica shells. The corresponding ZnO@SiO₂ core shell nanostructures are presented in Figure 3A–C, respectively. To weaken the influence of the encapsulation process on surface states of ZnO nanoparticles, the encapsulation process was conducted in absolute ethanol and at a mild pH value. From the TEM images, it was observed there was no obvious difference among the three ZnO@silica core shell nanostructures. The average size of the ZnO@silica core shell nanostructures was ~50 nm. The high-magnification TEM image of a single sphere (inset of each TEM image) clearly shows that ZnO nanoparticles have been successfully encapsulated with silica shells. Roughly, there were ~20 ZnO

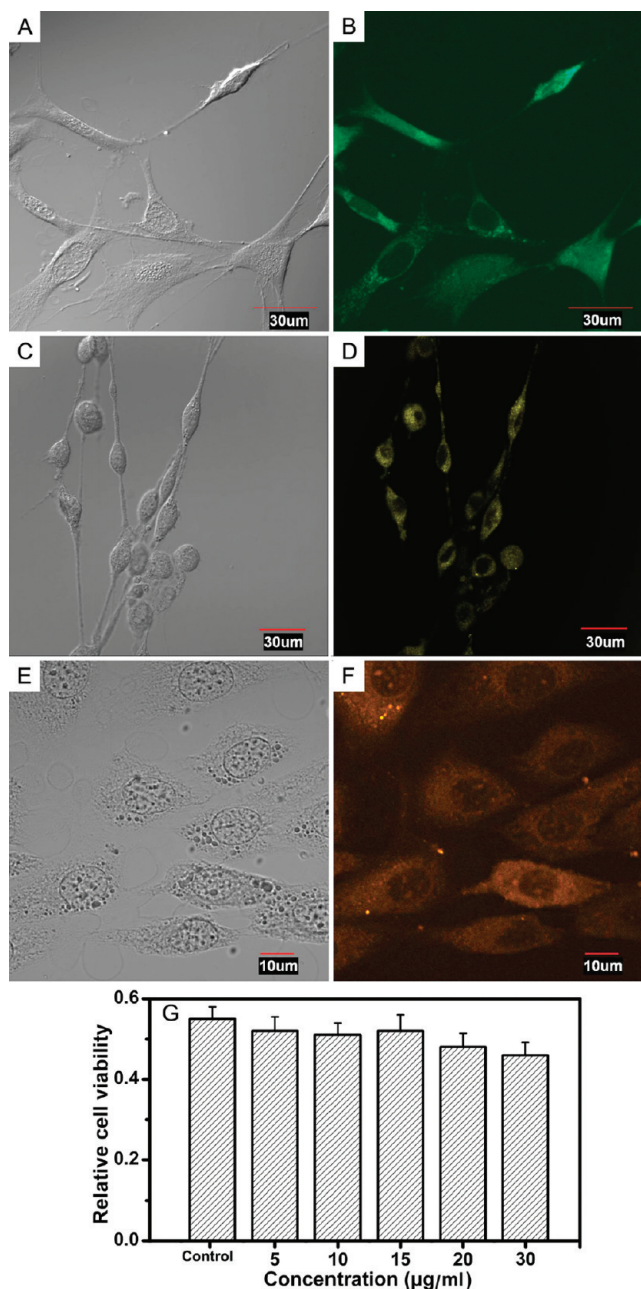


Figure 4. (A and B) DIC photograph and fluorescent image, respectively, of the cells labeled with ZnO@silica nanoparticles with green emission. (C and D) DIC photograph and fluorescent image, respectively, of the cells labeled with ZnO@silica nanoparticles with yellow emission. (E and F) DIC photograph and fluorescent image, respectively, of the cells labeled with ZnO@silica nanoparticles with orange emission. (G) Cell viability of incubated NIH/3T3 cells with increasing concentrations of ZnO nanoparticles for 24 h. Cell viability was measured using the MTT assay.

nanoparticles in each silica sphere. The PL spectra (Figure 3D) show that the photoluminescence properties of the ZnO nanoparticles were well preserved after they had been coated with a silica shell. The quantum yields of the ZnO@silica core shell nanoparticles were measured to be 18, 20, and 12% for the green, yellow, and orange emissions, respectively. The decrease in the quantum yields of the core shell nanoparticles as compared to the pure ZnO nanoparticles could be ascribed to the absorption of a photon by the silica shells. To improve the suspension stability of the ZnO@SiO₂ nanoparticles in

water, the obtained core shell nanoparticles were further modified with 3-[2-(aminoethyl)aminopropyl]trimethoxysilane (APTS) to introduce positively charged NH_2 groups. The surface charge of the modified core shell nanoparticles was measured to be ~ 30 mV. The positively charged ZnO@silica nanoparticles could be well dispersed in water, forming stable colloid solutions. The water stability of the positively charged ZnO@SiO_2 nanoparticles was further studied under different aqueous conditions with pH values ranging from 4.5 to 11. We found that the ZnO@SiO_2 nanoparticles were stable in water solutions when the pH values of the solutions ranged from 4.5 to 9. When the pH value was above 9, the positively charged ZnO@SiO_2 nanoparticles were aggregated together and settled in several hours. The stability of the positively charged ZnO@SiO_2 nanoparticles in a PBS solution was also studied. We demonstrated that the obtained nanoparticles could be well suspended in PBS solutions for more than one week, showing their good stability in PBS solutions.

Figure 4 shows the differential interference contrast (DIC) photographs and fluorescent image of NIH/3T3 cells incubated with ZnO@silica nanoparticles with different emission wavelengths. As shown in Figure 4B, the green emission from the cells was clearly observed under the fluorescent microscope, indicating that ZnO@silica nanoparticles were successfully attached to the cell surface. The successful attachment of the ZnO@SiO_2 nanoparticles could be ascribed to their positive surface charges. The corresponding control experiment, in which the cells were incubated without addition of ZnO@silica nanoparticles, is shown in Figure S5 of the Supporting Information. Similarly, panels D and F of Figure 4 show yellow and orange emissions, respectively, with good

intensity signals. Furthermore, the cytotoxicity of the ZnO nanoparticles was measured using the MTT assay, and the results are shown in Figure 4G. We demonstrated that, after incubation for 24 h, more than 85% of the cells survived when the concentration of ZnO nanoparticles was $\leq 30 \mu\text{g/mL}$, suggesting that ZnO nanoparticles are quite safe to living cells. These results show that ZnO nanoparticles are very promising for applications in cell labeling.

4. Conclusions

In summary, ZnO nanoparticles with various emission colors of blue, green, yellow, and orange were successfully prepared by using a facile ethanol-based precipitation method. The emission color of the ZnO nanoparticles was readily tuned via adjustment of the pH of the precipitation solution. The as-synthesized ZnO nanoparticles were not stable in aqueous solutions. To stabilize the ZnO nanoparticles in water, we encapsulated the as-precipitated ZnO nanoparticles with silica shells to form ZnO@silica core shell nanostructures. The ZnO@silica core shell nanostructures exhibited good water stability, and the PL properties of the ZnO nanoparticles were well retained. The in vitro cell culture experiments indicated that the ZnO@silica core shell nanoparticles exhibited low cytotoxicity and promise in cell labeling applications.

Acknowledgment. This work was supported by the Singapore MOE's ARF Tier 1 funding (WBS R-284-000-072-112).

Supporting Information Available: Five additional figures. This material is available free of charge via the Internet at <http://pubs.acs.org>.